Received: 12 March 2024 | Revised: 27 May 2024 | Accepted: 30 May 2024

DOI: 10.1002/pol.20240198

RESEARCH ARTICLE

JOURNAL OF POLYMER SCIENCE WILEY

Self-healing and cell adhesion properties of dynamic and photo-crosslinking PEG-based dual networks soft hydrogels

Merve Yasar[1] | **Burcu Oktay**[2] | **Ajda Coker Gurkan**[3] | **Nilhan Kayaman Apohan**[2]

[1]Department of Chemistry, Marmara University, Institute of Pure and Applied Sciences, Kadikoy, Turkey

[2]Department of Chemistry, Marmara University, Istanbul, Turkey

[3]Department of Biology, Marmara University, Istanbul, Turkey

Correspondence
Nilhan Kayaman Apohan, Faculty of Science, Department of Chemistry, Marmara University, 34722 Goztepe, Istanbul, Turkey.
Email: napohan@marmara.edu.tr

Funding information
Council of Higher Education (YOK) of Turkey for the PhD scholarship, Grant/Award Number: 100/2000 program

Abstract

Self-healing involves an autonomic response that repairs damage to living systems. In this study, polyethylene glycol (PEG) underwent aldehyde-functionalization using the Albrigh Goldman oxidation technique. Flexible, dynamic crosslink points to encourage self-healing are generated by the formation of acylhydrazone bonds formed between long-chain PEG dialdehyde and adipic acid dihydrazide. Furthermore, methacrylated PEG was synthesized to support the polymer matrix through dynamic covalent bonds. The hydrogels exhibited self-healing within the first 4 hours at room temperature and after 24 h. hydrogels with mechanical performance close to the original were obtained. They have good tensile and elongation strength and are well-suited for interaction with living cells.

KEYWORDS

dynamic covalent bonding, self-healing, soft hydrogels

1 | INTRODUCTION

Hydrogels are three-dimensional hydrophilic materials composed of crosslinks formed by both physical and chemical bonds. They find extensive use in biomedical applications due to their notable biocompatibility and water absorption capabilities, allowing them to retain water content up to 1000% of their dry weight. However, their weak mechanical properties and irreversible bonds make them rigid and limit their usage. Additionally, finding non-toxic monomers that function effectively within specific pH and temperature ranges is crucial.[1–3]

Self-healing is the process of repairing damage to extend the lifetime of the material. Nowadays, it is widely used in biomedical applications as a prominent feature of hydrogels.[4,5] Self-healing exhibits both extrinsic and intrinsic traits.[6] Extrinsic self-healing entails encapsulating a self-healing agent within the polymer structure, releasing it upon damage, and catalyzing the healing process.[7] Intrinsic self-healing involves non-covalent interactions like ionic interactions, as well as covalent bonds such as Schiff-base and acyl hydrazone linkages.[8–10]

Schiff-base linkages are imine bonds composed of amine and aldehyde groups. They possess reversible properties and typically require acid catalysts. In comparison to conventional reactions, they operate under mild reaction conditions and do not form side products. This has contributed to their popularity in self-healing studies.[11,12] Ding et al. synthesized oxidized alginate as a dialdehyde source and modified chitin

with acrylamide as an amine source. The pH-sensitive hydrogel showed self-healing properties within an hour without outer effect and re-activated self-healing after freezing.[13]

Acyl hydrazone linkages are reversible bonds that form between the acyl hydrazide group and the aldehyde group. Adipic acid dihydrazide (ADH) is a bifunctional acyl hydrazide source often used as a biocrosslinker in self-healing studies.[14] Their capability to operate under physiological conditions makes them promising candidates for future biomedical applications and tissue engineering studies.[15,16] Despite the abundance of amine sources used in self-healing investigations, there is still room for advancement in the production of better materials due to the lack of aldehyde sources. In acyl hydrazide studies, polysaccharides such as hyaluronic acid, dextran and alginate are predominantly functionalized with aldehyde groups through oxidative cleavage.[16–18] Su et al. studied oxidized hyaluronic acid and ADH to create a self-healing hydrogel without the need for a catalyst or initiator.[19] Wang et al. synthesized an injectable hydrogel containing gelatin, oxidized alginate, and ADH, which exhibited self-healing properties within a few minutes.[18]

Polyethylene glycol (PEG) is a water-soluble, biocompatible material that can be easily modified. Diacrylates of PEG can be synthesized in various molecular weights, providing an opportunity to control the strength of hydrogels.[20,21] Zhang et al. synthesized a pH-sensitive injectable hydrogel by using functionalized agarose with ethylene diamine and dialdehyde functionalized PEG. This hydrogel demonstrates self-healing ability within an hour at room temperature with 80% vitality.[22]

Gelatin is derived from the denaturation of collagen and serves as a widely utilized biocompatible amine source in self-healing studies.[23–26] Chen et al. successfully synthesized an injectable self-healing hydrogel by incorporating oxidized dextran, ADH and aminated gelatin with dynamic imine and acylhydrazone bonds.[17] However, the weak mechanical properties require either modification or the addition of supportive materials.[27]

In this study, a method was employed to dialdehyde-functionalize PEG1500 without the use of 4-formyl benzoic acid. This resulted in the formation of long acyl hydrazone bonds, creating adaptable and dynamic crosslink sites that encourage self-healing. Furthermore, PEG1500 was methacrylated to reinforce the polymer network. The hydrogels composed of dialdehyde functionalized PEG1500 and methacrylated PEG 1500 exhibited self-healing capabilities within a 24-hour timeframe, demonstrating commendable elongation and tensile strength. Additionally, MTT test confirmed their suitability for use with living cells.

2 | EXPERIMENTAL

2.1 | Materials

PEG1500, DMSO, chloroform, acetic anhydride, diethyl ether, dichloromethane (DCM), triethylamine (TEA), gelatin ADH, N-hydroxyethyl acrylamide, methylene bisacrylamide (MBA) and 2-hydroxy-2-methylpropiophenone (Darocur1173) (97%) were sourced from Sigma Aldrich. BUGAMED Biotechnology, TÜRKYE kindly provided collagen Type I (95%) from bovine tendon.

2.2 | Characterizations

The PEG1500-dialdehyde, PEGDA1500, as well as the hydrogels underwent characterization through Fourier-transform infrared spectroscopy (FT-IR) employing a Perkin Elmer ATR-FTIR Spectrometer. The samples were recorded directly within the range of 4000 to 600 cm^{-1}. The structure of PEG1500-dialdehyde and PEGDA1500 were confirmed through Varian Gemini 400 MHz proton nuclear magnetic resonance spectroscopy (^{1}HNMR) using deuterated chloroform.

Differential scanning calorimetry (DSC) analysis was carried out using a Perkin Elmer Diamond DSC. To eliminate impurities, the hydrogels were immersed in distilled water for an extended period, followed by a two-day drying process in an oven until a stable weight was reached. The first run was conducted from −30 to 150°C followed by a second run from −30 to 200°C, both at a heating rate of 10°C/min.

Tensile tests were performed using the Zwick Z010 Universal Tensile Test Machine at a fixed crosshead speed of 40 mm/min^{-1} at room temperature. Rectangular samples with dimensions of $50\times5\times1$ mm^3 were prepared for the tests, which were repeated at least three times.

For SEM imaging of hydrogels, a ZEISS EVO MA10 was employed.

2.3 | Synthesis of PEG1500-dialdehyde

PEG1500-dialdehyde was prepared by the relevant article from the literature 28. PEG1500 was first dissolved in DMSO, followed by the addition of chloroform and acetic anhydride. The mixture was stirred for 12 h at 500 rpm. The resulting product was precipitated in cold diethyl ether and subsequently dried under a vacuum overnight.

The yield is 70%. The reaction scheme is displayed in Figure S1.

2.4 | Synthesis of PEGDMA-1500

PEGDMA-1500 was prepared by the relevant article from the literature 29. PEG1500 was dissolved in DCM. Methacrylic anhydride was added dropwise under inert conditions at 250 rpm. Afterwards, TEA was added dropwise into the solution and mixed for 4 days. The resulting product was participated in cold diethyl ether. The yield is 80%. The reaction scheme is displayed in Figure S2.

2.5 | Synthesis of acylhydrazone-based hydrogel

Gelatin was dissolved in water at 40°C. Then, PEG1500-dialdehdye, PEGDMA-1500, ADH, and N-hydroxyethyl acrylamide were introduced into the solution. Following this, MBA and Darocur 1173 were added as photoinitiators. The reaction proceeded under UV light for 15 minutes to synthesize the hydrogel. In Table 1, the compositions of the hydrogels are listed. Figure 1 shows the monomer structures and molecular interaction creating the hydrogel.

2.6 | Hydrogel characterization

The hydrogel samples underwent overnight freeze-drying and were then weighted (W_d) to establish the gel content. Afterwards, the dried samples were immersed in deionized water for a night to eliminate uncrosslinked components. The samples were freeze-dried in freeze-dried once more and weighted (W_g). The gel content was calculated from Equation (1):

$$Gel\,Content\% = \frac{W_g}{W_d} \times 100\%. \quad (1)$$

The hydrogel samples were uniformly cut and their weight noted as W_1. They were then soaked in ethanol overnight to assess the porosity. Afterward, any excess ethanol was removed by filter paper, and the hydrogels were reweighted as W_2. The porosity was calculated using Equation (2):

$$Porosity\,(\%) = \frac{W_2 - W_1}{V\rho} \times 100\%, \quad (2)$$

where V was the volume of hydrogels and ρ was the density of ethanol.

The hydrogel samples were soaked in deionized water for an entire night to eliminate any unreacted monomers.

TABLE 1 Compositions and gel contents of hydrogels.

No	Gelatin (g)	ADH (g)	PEG1500-dialdehyde (g)	PEGDMA-1500 (g)	NHEA (g)	MBA (g)
GA-0	0.2	0.02	0.2	0.11	0.3	0.005
GA-1	0.2	0.04	0.2	0.11	0.3	0.005
GA-2	0.2	0.06	0.2	0.11	0.3	0.005
GA-2-1	0.2	0.06	0.4	0.11	0.3	0.005
GA-2-2	0.2	0.06	0.6	0.11	0.3	0.005

Abbreviations: ADH, adipic acid dihydrazide; MBA, methylene bisacrylamide; PEG, polyethylene glycol.

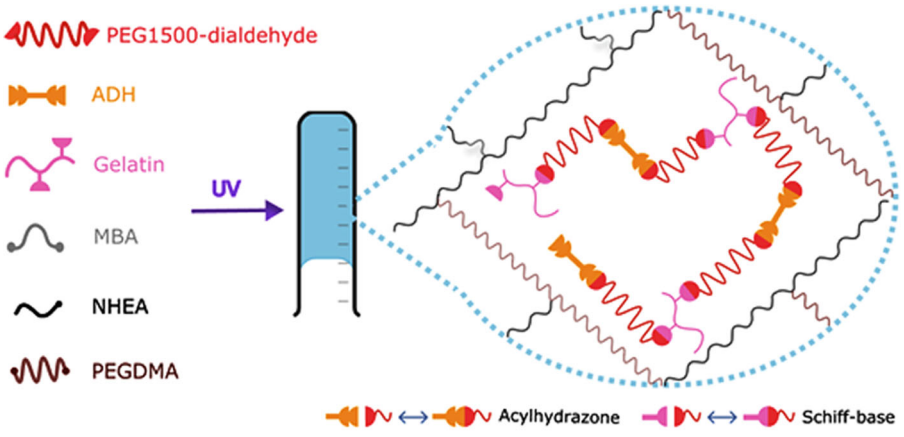

FIGURE 1 Hydrogel preparation pathway.

Following this, the samples underwent an overnight freeze-drying process and the weight of the dry hydrogel was recorded as W_d to calculate the swelling ratio. The hydrogel samples were then immersed in distilled water at room temperature for varying time intervals ranging from 5 to 2880 minutes, and weight was noted as W_s. Throughout the measurements, any excess water was removed with filter paper. These swelling tests were repeated in triplicate. The swelling ratio was calculated from Equation (3):

$$SR = \frac{W_s - W_d}{W_d} \times 100\%, \quad (3)$$

where SR: Swelling ratio.

In order to determine the pH dependent swelling behavior of hydrogels, the hydrogel specimens were freze-dried overnight and their dry weight recorded as W_d. Following drying, they were placed in buffer solution with pH values of 2, 4.5, 7, 8, and 10 at room temperature and their swollen weigh at equilibrium state was recorded as Ws. The pH dependent swelling ratio was determined using Equation (3).

2.7 | Self-healing ability

Self-healing capability of the hydrogel was done by examining the tensile strength of the hydrogel sample before and after the healing process. The hydrogel sample was split into two pieces and then carefully rejoined with slight handling pressure, allowing it to mend overnight at room temperature. The test was repeated at least three times for accuracy. The healing efficiency (SH_{eff}) was determined by comparing the tensile strength of healed sample to that of the original one.

2.8 | Cell growth and viability studies

Human embryonic kidney 293 cells (HEK293; ATCC: CRL-1573) were employed in the study. 3-(4,5-Dimethylthiazol-2-yl)-2,5-Diphenyltetrazolium Bromide (MTT) reagent from NeoFroxx (1334), was used to assess cell viability. Collagen-coated hydrogel scaffolds were fabricated by applying 4 μg of Type I collagen, dispersed in a 0.1 M acetic acid solution, onto the hydrogel surface. These treated scaffolds were then allowed to incubate at room temperature overnight. Afterwards, the hydrogels were cut into uniform pieces, each measuring $1 \times 1\ cm^2$ for each well, and they were sterilized under UV for at least 1 h. The cells were then seeded into 24 well plates and exposed to the hydrogels for 24 h. Next, the samples were removed and MTT reagent was introduced into each well at a final concentration of 0.1 mg/mL. The cells were further incubated for 4 h at 37°C in a 5% CO_2 incubator until formazan crystals were visible under microscopy. Subsequently, the media were discarded and 200 μL DMSO was added to each well. Absorbance values were read at 570 nm using Agilent BioTek Cytation-C-10. Cell viability was calculated according to Equation (4):

$$Cell\ Viability\% = \frac{Mean\ absorbance\ of\ the\ treatment}{Mean\ absorbance\ of\ the\ control} \times 10. \quad (4)$$

Bright field images of the cells were taken by Zeis Axio ZI Invert Microscope.

2.9 | Cell fixation

HEK293 cells were placed in 24 well plates and exposed to hydrogels for 24 hours. The hydrogels were then taken out and rinsed with 1x PBS. Next, they were fixed using 1 mL of 2.5% glutaraldehyde (GA) for 2 h. at room temperature. Subsequently, the hydrogels were washed with 1× PBS to remove excess GA. The fixated hydrogels were gradually immersed in increasing concentrations of ethanol, with a 10% increase at each step, over a span of 10 minutes (ranging from 50% to 100%). The hydrogels were stored at −20°C until they underwent SEM analysis.

3 | RESULTS AND DISCUSSIONS

3.1 | Characterization of PEG1500-dialdehyde

The synthesis reaction of PEG1500-dialdehyde was proceeded by the Albrigh Goldman oxidation method, resulting in a high yield with excess acetic anhydride as shown in Figure S3. DMSO served dual roles as both the solvent and reactant. Initially, DMSO reacted with acetic anhydride, forming sulphonium ions. Then, a secondary reaction ensued involving primary alcohol. As a byproduct, acetic anhydride split into two components. Finally, an elimination reaction led to the formation of the desired product.[30,31] The product was characterized by FTIR and ^{1}HNMR spectroscopy techniques.

Figure 2 displays the FTIR spectra of PEG and PEG1500-dialdehyde. In Figure 2A, it is evident that the

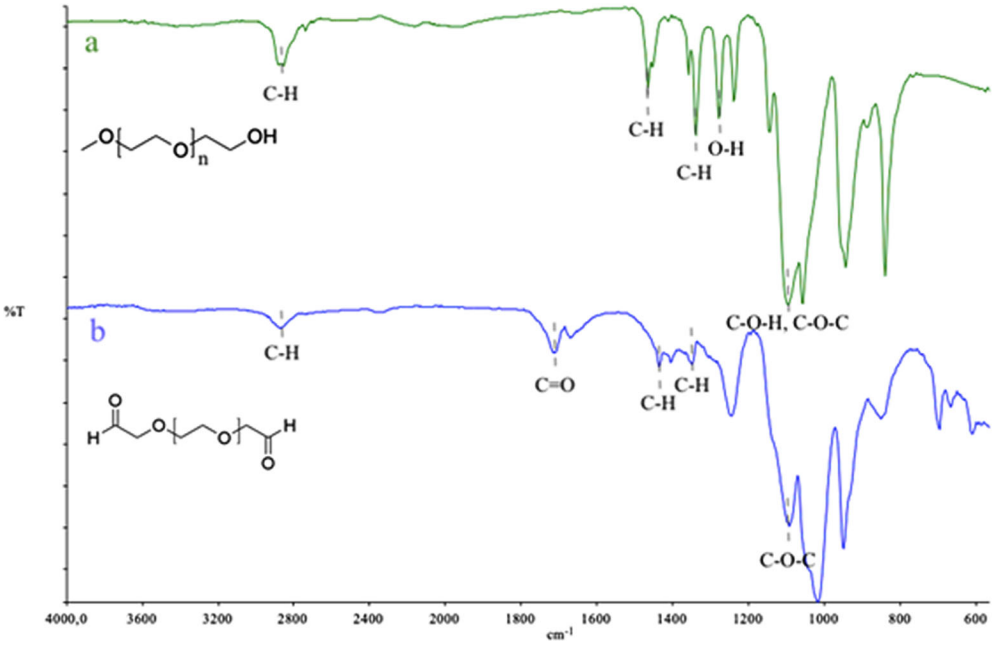

FIGURE 2 Fourier-transform infrared spectroscopy (FTIR) spectra of PEG1500-dialdeyde. (A) Polyethylene glycol (PEG), (B) PEG1500-dialdeyde.

C—H aliphatic chain stretching occurs at 2856 cm^{-1}, with C—H bending stretching at 1466 cm^{-1} and 1340 cm^{-1}. The O—H and C—O—H stretching peaks are observed at 1278 cm^{-1} and 1096 cm^{-1} respectively, indicative of PEG.[32]

Figure 2B presents the FTIR Spectrum of PEG1500-dialdeyde. The C-H aliphatic stretching and bending vibrations belongs to PEG are detected at 2871 cm^{-1}, 1466 cm^{-1}, and 1340 cm^{-1} respectively. Additionally, C—O—C stretching vibrations are evident at 1018 cm^{-1}. Notably, a prominent aldehyde peak is observed at 1716 cm^{-1}, providing evidence of successful completion of the reaction.

The ^{1}HNMR Spectrum of PEG1500-dialdehyde is depicted in Figure 3. The triplet at 2.9 ppm corresponds to the methylene protons (CH_2) located between the ether chains (C). A small triplet at 9.1 ppm (A) indicates the presence of an aldehyde moiety due to long chain structure of PEG1500. The singlet at 3.9 ppm (B) is attributed to adjacent group of the aldehyde. The solvent peak is evident at 7 ppm.

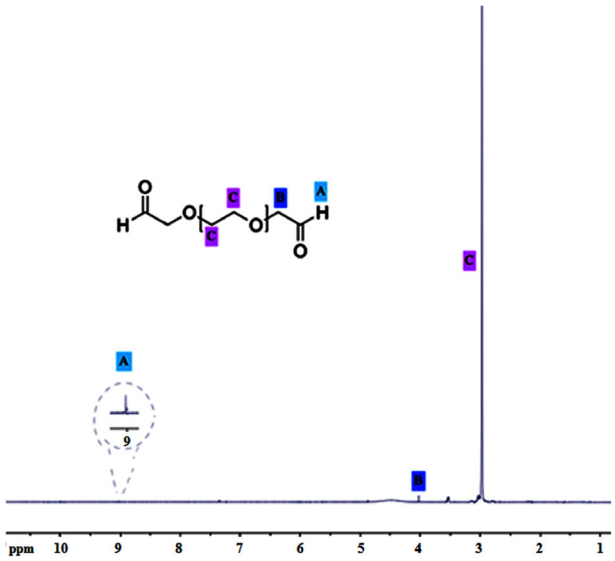

FIGURE 3 Proton nuclear magnetic resonance spectroscopy (^{1}HNMR) spectrum of PEG1500-dialdehyde.

3.2 | Characterization of PEGDMA-1500

PEGDMA-1500 was synthesized through a reaction between acid anhydride and the hydroxyl group of PEG, similar to the process used for acyl chloride to ester synthesis. The reaction mechanism is illustrated in Figure S4. Initially, the hydroxyl group of PEG, act as a nucleophile and attacks the carbonyl group of methacrylic anhydride. This interaction was followed by protonation via TEA, a weak base. The negatively charged oxygen then underwent closure, causing methacrylic acid to leave, resulting in the formation of the ester. Consequently, a carboxylic acid was produced as a side product rather than HCl.[29] PEGDMA-1500 was characterized via FTIR and ^{1}H-NMR.

The FTIR Spectrum of PEGMA1500 is presented in Figure 4. The ester peak at 1713 cm^{-1} (C═O) and (C═C) stretching at 1636 cm^{-1} demonstrate that the reaction was completed.

The ^{1}HNMR Spectrum of PEGDMA-1500 is shown in Figure 5. The singlet at 1.9 ppm (C) corresponds to the methyl groups of methacrylate functionality. The triplet at 3.6 ppm belongs to the methylene protons of the polyether.

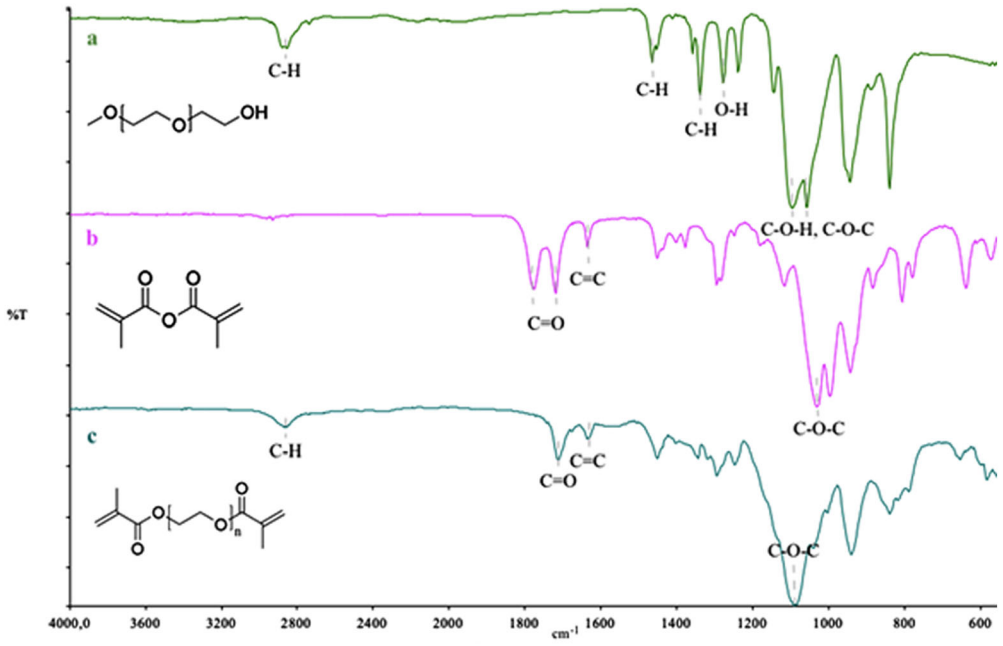

FIGURE 4 Fourier-transform infrared spectroscopy (FTIR) spectra of PEGMA-1500. (A) PEG, (B) methacrylic anhydride, (C) PEGDMA-1500.

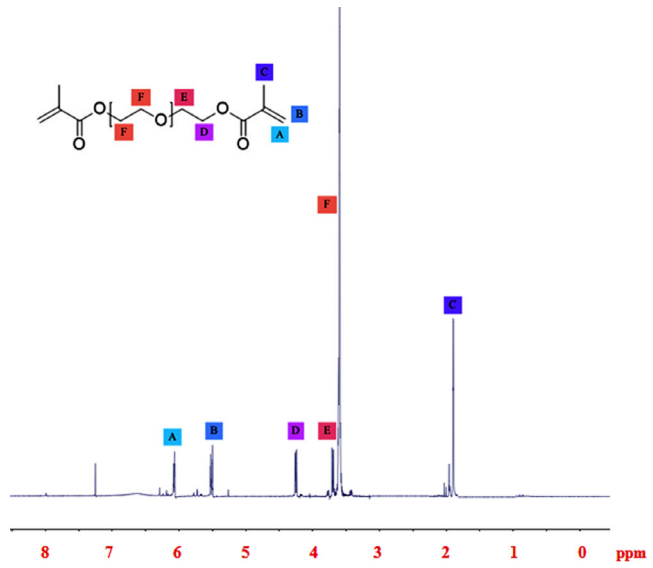

FIGURE 5 Proton nuclear magnetic resonance spectroscopy (^{1}HNMR) spectrum of PEGDMA-1500.

Additionally, the peaks at 3.7 ppm (E) and at 4.2 ppm (D) belong to methylene protons adjacent to PEG and methacrylate, respectively. The doublets at 5.5 ppm and 6.1 ppm (A, B) serve as evidence of the attachment of the vinyl group.

3.3 | Synthesis of acylhydrazone-based hydrogel

In the study, the synthesis of network structures was successfully accomplished by two distinct mechanisms. The first one, radical copolymerization, played a crucial role in establishing enduring covalent bonds, thereby supporting the mechanic stability of the matrix. This process involved the decomposition of the initiator under UV light, which then proceeded to attack the vinyl groups of NHEA, PEGDMA-1500 and MBA to initiate the formation of a polymer chain. The second one involved in dynamic bonds, facilitating self-healing following damage. This was accomplished through the formation of a dynamic imine bond, resulting from a condensation reaction between the amine group of gelatin and the aldehyde group of PEG1500-dialdehyde. Additionally, an acyl hydrazone dynamic bond formed between PEG1500-dialdehyde and ADH.

The FTIR spectra of GA-0, GA-1, GA-2, and GA-2-2 are shown in Figure S5. In the spectra of all three hydrogel samples compare to Figure S5C, the N—H stretching peak at 3278 cm^{-1} was weakened due to the occurrence of an imine bond. A new C—O—C peak emerged at 1056 cm^{-1}, attributed to the presence of PEG chains. The disappearance of C═C double bond stretching peak at 1636 cm^{-1} and 815 cm^{-1} indicates the completion of the UV curing reaction. Moreover, the C═O stretching at 1626 cm^{-1} and the N—H bending peak at 1560 cm^{-1}, characteristics of acylhyrazone, are depicted in Figure S5B. The aldehyde peak of PEG1500-dialdehyde at 1716 cm^{-1}, disappeared in GA-0, GA-1, and GA-2. For all hydrogels, the amide II band (N—H) belongs to gelatin around 1530 cm^{-1} shifted and increased in intensity which can be attributed to the formation of the C═N hydrazone bond. In the spectrum of GA-2-2 (Figure S5G) the intensity of peaks at 1343 cm^{-1} (C—H) and 1108 cm^{-1} (C—O—C) increased with the higher PEG-dialdehyde ratio in the hydrogel.

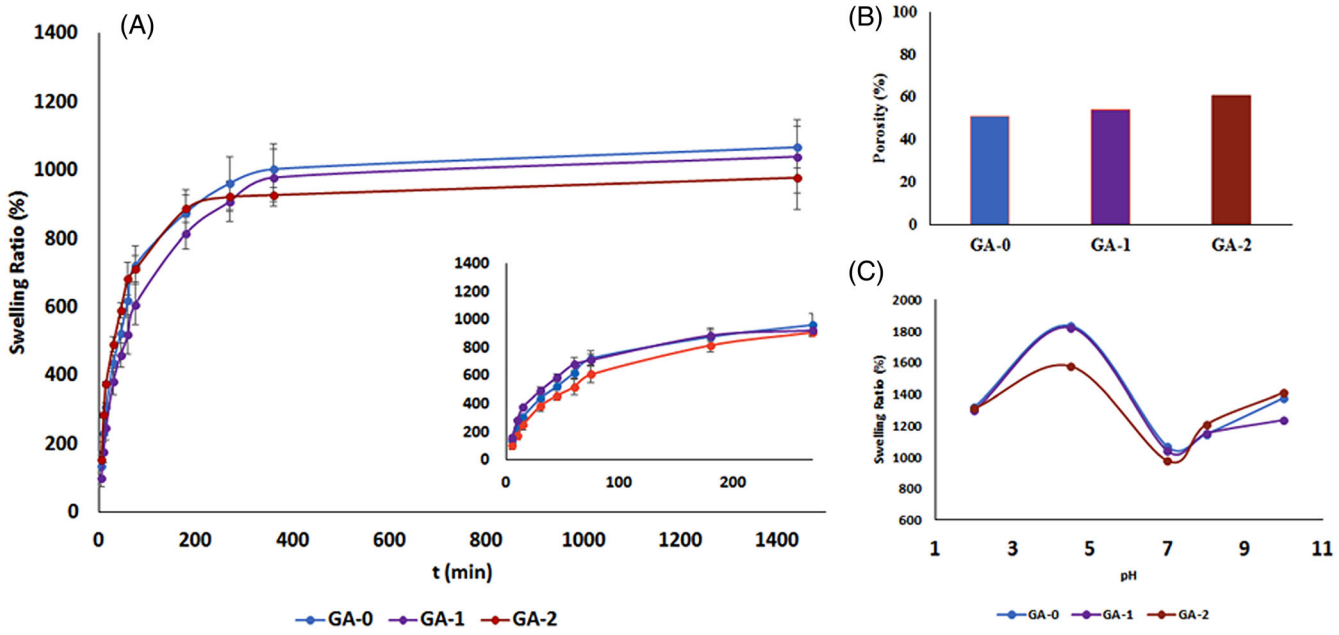

FIGURE 6 Hydrogel swelling behavior of GA-0, GA-1, GA-2. (A) Swelling kinetics at pH = 7, (B) porosity (C) equilibrium swelling within different buffer solutions, (C) equilibrium swelling within different buffer solutions.

3.4 | Swelling behaviors of hydrogels

The swelling profiles of GA-0, GA-1, and GA-2 are given in Figure 6A. The hydrogel exhibits swelling as a result of the presence of hydrophilic monomers and oligomers within the cross-linked polymer matrix. The presence of functional groups like amine, carbonyl, amide, and hydroxyl in both monomers and resins, along with the ether repeats of the PEG chain, contribute to the swelling behavior. Therefore, polar interactions, hydrogen bonds, and the diffusion of water molecules through cross-linkers, driven by osmotic pressure, lead to the swelling of the gel. As shown in Figure 6A, the hydrogels exhibit a swelling capacity of up to 1000 times their dry weight. The hydrogels demonstrated similar swelling trends in the first 4 hours, with the primary influencing factor being the ADH content. Increasing the ADH content from GA-0 to GA-2 was expected to enhance acyl hydrazone bonds. Increasing dynamic crosslinks increases the number of crosslinking points and consequently reduces the swelling ratio. In a study conducted by Liu and coworkers, ADH was modified in hyaluronic acid through EDC. They similarly reported that an increase in ADH led to a decrease in the swelling ratio, attributing this effect to the cross-linker.[33] Li et al. investigated the impact of the ADH ratio on swelling and crosslink density. The swelling ratio showed a decreasing trend with increasing ADH content.[34] Notably, GA-2 reaches equilibrium faster than others within 4 hours. This is attributed to its more porous structure, which enables faster water absorption and facilitates a faster interaction between water molecules and ADH.

TABLE 2 Gel content of acylhydrazone-based hydrogels.

No	Gel content (%)
GA-0	72
GA-1	70
GA-2	66
GA-2-1	57
GA-2-2	55

The gel content of the hydrogels is presented in Table 2. With an increase in ADH ratio from GA-0 to GA-2, the gel content decreased from 72% to 68%. The network structure of the hydrogel comprises both covalent cross-links, which are highly resistant to water-induced swelling, and dynamic covalent bonds that contribute to cross-linking but can be broken down over prolonged water exposure. As a result, during the equilibrium swelling experiment, dynamic bonds might break, leading to the removal of hydrophilic components. This provides a plausible explanation for the observed reduction in gel content. Conversely, the porosity increased from 50% to 60% from G-0 to G-2.

Figure 6B provides a visual representation of the porosity data. That may be related to the diffusion of the ethanol-soluble parts and increasing the gaps between crosslinkers. These results show that dynamic crosslinks are weaker than their covalent counterparts, making them susceptible to decomposition and

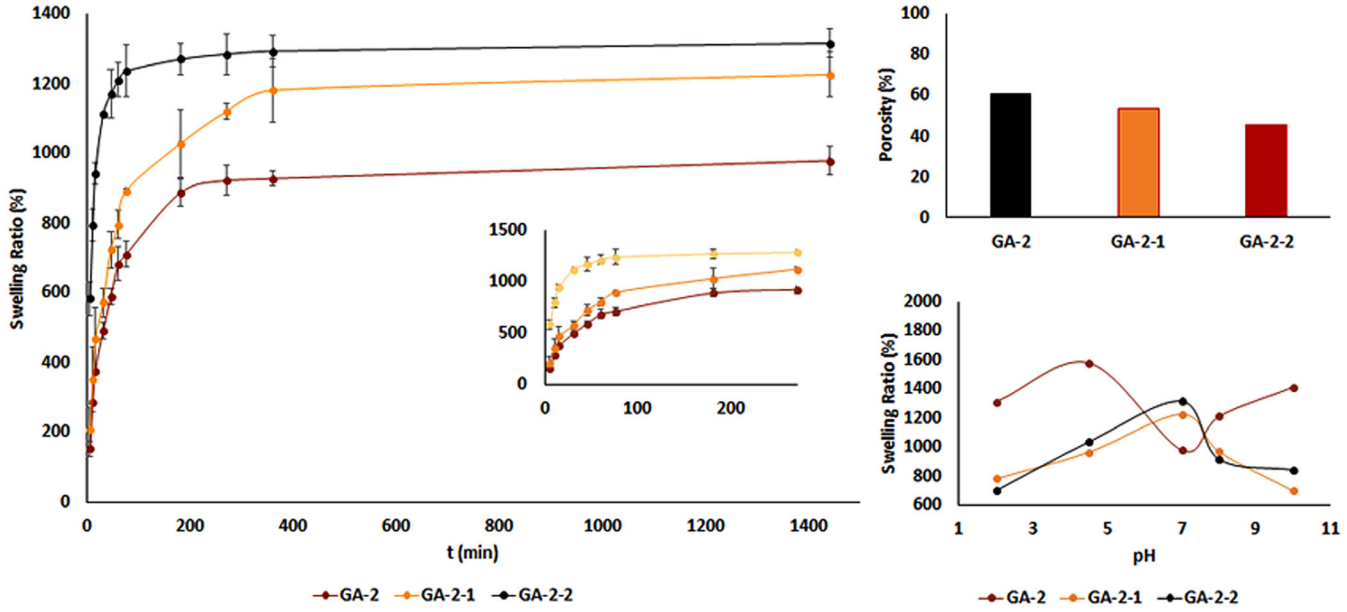

FIGURE 7 Hydrogels swelling behavior GA-2, GA-2-1, GA-2-2. (A) Swelling kinetics at pH = 7, (B) porosity, (C) equilibrium swelling within different buffer solutions.

subsequent departure from the polymer matrix after prolonged exposure to solvents. When comparing swelling ratios over 24 hours, it was observed that the hydrogel with a lower ADH content container (GA-0) exhibited greater swelling than expected.

Figure 6C displays the swelling behaviors of hydrogels in various buffer solutions. The hydrogels possess an amphoteric nature as they contain amine, amide, and carboxylic groups. At pH = 4, free amine groups protonate, and positive charges repel each other, leading to swelling. It was previously reported that despite acyl hydrazone and Schiff-base linkages being pH sensitive, no sol–gel transition in the polymer matrix was observed.[35] The gel integrity was maintained through covalent bonds formed via radical polymerization, so the hydrogels show pH resistance. Compared to pH = 4, decreasing swelling trends at pH = 4, show that acyl hydrazone decomposes at pH <4, and protonated amine groups create ion pairs with mobile anions and shrink the gels.

Hydrogels reached equilibrium at pH 7. At higher pH, amine groups neutralize, while carboxylic acids deprotonate resulting in repulsion between negative charges. Hence, water intake increases. Since the amine group is the dominant, the highest swelling ratio occurred at lower pH. The swelling ratio in both acidic and basic mediums was higher than in a neutral environment. Similar to what Yu Su and colleagues previously reported, we observed that GA-2, which contains a higher ADH content, exhibits a lower swelling rate. This can be attributed to the slower hydrolysis rate of the acyl hydrazone bond compared to GA-0 and GA-1. As a result, the dynamic crosslinker intensity is higher in GA-2 which causes a lower swelling ratio.[19,36]

TABLE 3 Glass transition temperature of acylhydrazone-based hydrogels.

No	Tg_1	Tg_2
GA-0	8	58
GA-1	25	69
GA-2	28	73
GA-2-1	−12	13
GA-2-2	–	34

Figure 7A displays the results of swelling behavior. As previously reported, low crosslink density, the molecular weight of PEG chains, and hydrophilic ether structure cause a high swelling degree.[36] Compared to GA-2 to GA-2-2, the only variable is PEG dialdehyde. It is expected that increasing PEG-dialdehyde leads to an increase in dynamic crosslinks and a decrease in swelling degree. However, the effect of hydrophilic PEG chains is more dominant than that of crosslink points. Thus, from GA-2 to GA-2-2, swelling ratios increased.

Hydrogel porosities are shown in Figure 7B. The porosity decreases from 60% to 45% in hydrogels from GA-2 to GA-2-2. GA-2-1 and GA-2-2 have lower porosity because aldehyde groups create dynamic crosslinks, and PEG chain entanglements. Increasing PEG-dialdehyde decreases gel content from 66% to 55%. It can be explained that prolonged exposure to water decomposes

TABLE 4 Acyl hydrazone-based hydrogels mechanic test results.

	Original			Self-healed			
Samples	E-modul (N/mm^2)	Tensile strength (MPa)	Elongation at break (%)	E-modul (N/mm^2)	Tensile strength (MPa)	Elongation at break (%)	(SH_{eff})* (%)
GA-0	22	16	194	14	14	135	90
GA-1	9	27	310	6	15	200	54
GA-2	9	36	145	14	7	115	20
GA-2-1	15	15	226	23	11	227	74
GA-2-2	14	10	285	21	11	232	103

the dynamic bonds and the soluble parts pass into the water phase.

In Figure 7C, pH-dependent swelling tests were presented. At pH above and below neutrality, different swelling behaviors were observed. Under neutral conditions, the swelling ratio follows the trend GA-2 < GA-2-1 < GA-2-2 due to the increased concentration of PEG-dialdehyde and the dominant effect of the hydrophilic PEG chain. The increase in PEG-dialdehyde concentration from GA-2 to GA-2-2 enhanced imine and acyl hydrazone linkages resulting in a lower swelling ratio at both low and high pH values compared to neutral conditions. At lower pH, protonated groups paired with free ions, contributing to hydrogel shrinkage. Conversely, at higher pH, ether bonds become polarized and form ion pairs with free cationic ions, causing a decrease in the degree of swelling. Due to their polar nature, hydrolyzed acyl hydrazone and aldehyde groups interacted with free protons, causing the hydrogel to shrink.

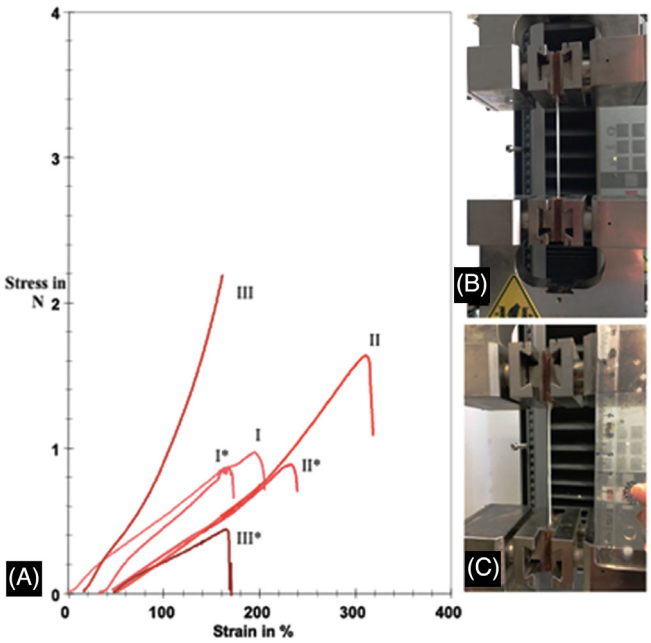

FIGURE 8 Acylhydrazone-based hydrogels stress–strain curves. I: GA0, II: GA-1, III: GA-2. (A) Original, (B) self-healed GA-1.

3.5 | Thermal behaviors of acylhydrazone-based hydrogels

The glass transition temperature (Tg) of acyl hydrazone-based hydrogels was given in Table 3. Two different Tg values were observed. The first Tg belongs to PEGDMA-1500 and PEG1500-dialdehyde polyether chains. Gelatin has Tg around at 50 to 60°C. From GA-0 to GA-2, increasing dynamic bonds prevent motion and increase Tg. Coherently with tensile strengths, from GA-2 to GA-2-2, increasing the PEG chain creates space and decreases both T_g values.

3.6 | Mechanical behavior of acyl hydrazone based hydrogels

The mechanical test results of acyl hydrazone-based hydrogels are shown in Table 4. Mechanical test results of GA-0, GA-1, and GA-2 are shown in Figure 8. Pure gelatin displays low-mechanical properties.[37] ADH forms an acyl hydrazone dynamic bond with an aldehyde, creating crosslinking sites. Therefore, the mechanical properties of the prepared hydrogels are seen to be more advanced than pure gelatin. As the ADH content increases, so do the crosslinking sites, resulting in higher tensile strength. As seen in Table 4 the tensile strength increased from 16 MPa to 36 MPa. On the other hand, the increasing crosslink points increase molecular interaction, while reducing elongation. In the GA-2 sample, the elongation decreased to 145% due to the efficient increase in dynamic crosslink density, despite the increasing PEG content.

A similar effect can be observed in the self-healing version. The tensile strength of self-healed hydrogels increased from GA-0 to GA-1 while decreased in GA-2. Intense molecular interactions prevent the re-bound of broken bonds due

to the intensity of the polymer matrix. GA-2 has 20% self-healing efficiency. The mechanical properties of PEG/gelatin-based hydrogels after the self-healing process have shown similarities with the results reported in the literature. Hydrogels typically exhibit nearly identical mechanical properties both before and after the healing process.[38]

Mechanical test results of GA-2, GA-2-1, and GA-2-2 are shown in Figure 9. It has been reported that the long chains of PEGDMA-1500 increased the distance between crosslink points and decreased crosslink density in the polymer matrix.[36] Increasing the amount of PEG1500-dialdehyde increased dynamic acyl hydrazone bonds and improved tensile strength. When the PEG1500-dialdehyde amount exceeded that of ADH, excess PEG1500-dialdehyde could potentially bond with amine groups in gelatin, leading to molecular interactions via polar interactions and H-bonds. However, increasing PEG1500-dialdehyde did not improve tensile stress due to long chains in the matrix, even if it increased acyl hydrazone bonds. As expected, the elongation increased from GA-2 to GA-2-2. In self-healed hydrogels, broken bonds have the space to move and are easy to re-bond due to long chains in the polymer matrix. Thus, they exhibit higher tensile stress compared to GA-2. The elongations of both hydrogels and self-healed hydrogels improved with increased PEG-aldehyde content. PEG can reorganize the polymer matrix, imparting flexibility to the hydrogels.[39] Hwang et al. similarly reported about poly(ethylene glycol) (PEG)-based bioadhesives.[39] In comparison to the original and self-healed hydrogels, the tensile stress of self-healed hydrogels slightly decreased. The notable result for GA-2-2 is a 103% self-healed efficiency, which may be attributed to the excess PEG1500-dialdehyde providing more opportunities for bonding.

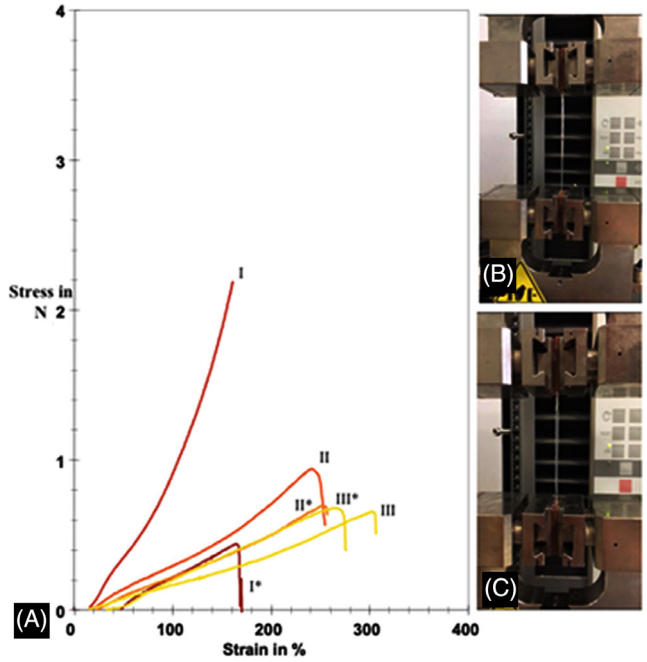

FIGURE 9 Acylhydrazone-based hydrogels stress–strain curves. I:GA-2, II:GA-2-1, III: GA-2-2. (A) GA-2-2 original, (B) GA-2-2 self-healed.

3.7 | Self-healing behavior of acylhydrazone-based hydrogel

The mechanical test results of self-healed hydrogels are given in Table 4. Both the original and self-healed samples exhibited comparable performance, demonstrating reversible bonds improved elongation. The self-healed hydrogel proved to be equally as effective as its original counterpart. In Figure S6, optic microscope images illustrate the self-healing phases. The hydrogel was cut in half

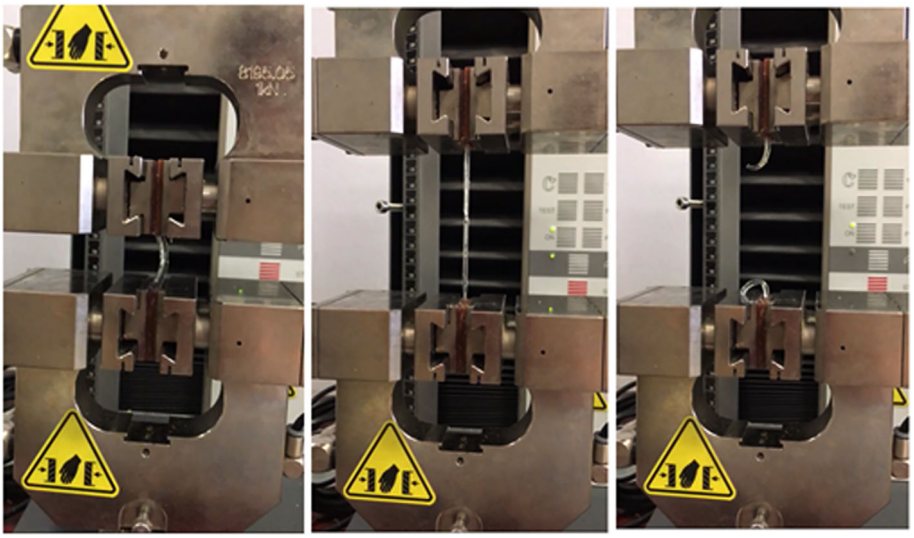

FIGURE 10 Digital images of the GA-2 hydrogels during tensile fracture test.

and re-connected at room temperature. The hydrogel started to heal the crack in 4 h. Figure 10 shows photographs from the mechanical tests conducted on GA-2 after 24 h. self-healing period. As can be seen, the hydrogel was successfully extended to the fracture point by self-healing.

3.8 | In-vitro studies of acylhydrazone-based hydrogels

In Figure S7, MTT tests were conducted on hydrogels with and without collagen. Test results for 24 h indicated that the hydrogels were not toxic for cells. Viability increased from 117% to 169% after collagen was applied to the surface of the hydrogel. Collagen promoted cells adhesion to the hydrogel. Additionally, optic microscope images at 10× magnification were presented in Figure S8. Compared to the control, HEK293 cells maintained vitality on the hydrogel surface after 24 h.

Figure S9 shows SEM images of HEK293 cells fixated hydrogels. As can be seen, the cells are adhered and well-spread on the hydrogel surface. They adhered effectively on the collagen coated hydrogel, despite its irregular surface. Hence, it can be concluded that the hydrogel provides a suitable support for cells attachment.

4 | CONCLUSION

In this study, a self-healing hydrogel with acyl hydrazone bond was synthesized. PEG1500-dialdehyde served as a distinctive source of aldehyde, ensuring both flexibility and a dynamic reversible bond to the polymer matrix. Additionally, PEG1500-diacrylate was synthesized to reinforce the polymer matrix. The introduction of long PEG chains cause the swelling ratio reached up to 1000%. Conversely, an increase in acyl hydrazone bonds resulted in a decrease in the swelling ratio due to the increased crosslink points. The hydrogel exhibited pH-dependent features according to aldehyde and acyl hydrazone amounts. Notably, the hydrogel showed self-healing within 4 hours at room temperature. Subsequently, after 24 hours of healing, tensile tests demonstrated that the hydrogels repaired themselves to a degree close to the original state. Furthermore, the viability results obtained from MTT tests, spread, and proliferated cell images observed under optical and SEM microscope, collectively indicate that the hydrogel structure holds promise as a potential scaffold for HEK293 cells. The prepared hydrogels can be used as wound dressing and drug delivery systems in medicine and biomedical engineering. They can also be preferred in the field of cosmetics, food packaging, agriculture, and water purification systems.

ACKNOWLEDGMENTS

The author Merve Yasar acknowledges Council of Higher Education (YOK) of Turkey for the PhD scholarship of 100/2000 program.

CONFLICT OF INTEREST STATEMENT

The authors declare that they have no known competing financial interests or personal relationships that could have appeared to influence the work reported in this article.

DATA AVAILABILITY STATEMENT

Data will be made available on request.

ORCID

Nilhan Kayaman Apohan https://orcid.org/0000-0002-7750-3058

REFERENCES

[1] B. Oktay, N. Kayaman-Apohan, M. Süleymanoğlu, S. Erdem-Kuruca, *Mater. Sci. Eng. C Mater. Biol. Appl.* **2017**, *73*, 569.
[2] N. F. Mohd Sani, H. J. Yee, N. Othman, A. A. Talib, R. K. Shuib, *Polym. Test.* **2022**, *111*, 107598.
[3] A. K. Aslıhan Hilal Kurtoğlu, *J. Fac. Pharm.* **2009**, *38*, 211.
[4] F. Cadamuro, V. Ardenti, F. Nicotra, L. Russo, *Molecules* **2023**, *28*, 2851.
[5] W. Han, C. Chen, K. Yang, H. Wang, H. Xia, Y. Zhao, Y. Teng, G. Feng, Y. M. Chen, *Int. J. Biol. Macromol.* **2023**, *227*, 373.
[6] Y. Tu, N. Chen, C. Li, H. Liu, R. Zhu, S. Chen, Q. Xiao, J. Liu, S. Ramakrishna, L. He, *Acta Biomater.* **2019**, *90*, 1.
[7] Y. K. Song, T. H. Lee, J. C. Kim, K. C. Lee, S. H. Lee, S. M. Noh, Y. I. Park, *Molecules* **2019**, *24*, 1679.
[8] S. Wang, Y. Lv, S. Feng, Q. Li, T. Zhang, *Polym. Eng. Sci.* **2018**, *59*, 919.
[9] Y. Wang, Y. Chen, J. Zheng, L. Liu, Q. Zhang, *ACS Omega* **2022**, *7*, 12076.
[10] W. Zhang, K. Zhang, S. Yan, J. Wu, J. Yin, *J. Mater. Chem. B* **2018**, *6*, 6865.
[11] W. Li, B. Wang, M. Zhang, Z. Wu, J. Wei, Y. Jiang, N. Sheng, Q. Liang, D. Zhang, S. Chen, *Cellulose* **2020**, *27*, 2637.
[12] S. Li, M. Pei, T. Wan, H. Yang, S. Gu, Y. Tao, X. Liu, Y. Zhou, W. Xu, P. Xiao, *Carbohydr. Polym.* **2020**, *250*, 116922.
[13] F. Ding, S. Wu, S. Wang, Y. Xiong, Y. Li, B. Li, H. Deng, Y. du, L. Xiao, X. Shi, *Soft Matter* **2015**, *11*, 3971.
[14] C. G. França, D. P. Sacomani, D. G. Villalva, V. F. Nascimento, J. L. Dávila, M. H. A. Santana, *Eur. Polym. J.* **2019**, *121*, 109288.
[15] Z. Cimen, S. Babadag, S. Odabas, S. Altuntas, G. Demirel, G. B. Demirel, *ACS Appl. Polym. Mater.* **2021**, *3*, 3504.
[16] S. W. Kim, D. Y. Kim, H. H. Roh, H. S. Kim, J. W. Lee, K. Y. Lee, *Biomacromolecules* **2019**, *20*, 1860.
[17] M. Chen, J. Tian, Y. Liu, H. Cao, R. Li, J. Wang, J. Wu, Q. Zhang, *Chem. Eng. J.* **2019**, *373*, 413.

[18] L. Wang, F. Deng, W. Wang, A. Li, C. Lu, H. Chen, G. Wu, K. Nan, L. Li, *ACS Appl. Mater. Interfaces* **2018**, *10*, 36721.
[19] W. Y. Su, K. H. Chen, Y. C. Chen, Y. H. Lee, C. L. Tseng, F. H. Lin, *J. Biomater. Sci. Polym. Ed.* **2011**, *22*, 1777.
[20] N. C. Paxton, M. C. Allenby, P. M. Lewis, M. A. Woodruff, *Eur. Polym. J.* **2019**, *118*, 412.
[21] F. Della Sala, M. Biondi, D. Guarnieri, A. Borzacchiello, L. Ambrosio, L. Mayol, *J. Mech. Behav. Biomed. Mater.* **2020**, *110*, 103885.
[22] Z. Zhang, X. Wang, Y. Wang, J. Hao, *Biomacromolecules* **2018**, *19*, 980.
[23] X. Fan, J. Geng, Y. Wang, H. Gu, *Polymer* **2022**, *246*, 124769.
[24] M. Vahedi et al., *Macromol. Mater. Eng.* **2018**, *303*, 1800200.
[25] Y. Du et al., *Macromol. Biosci.* **2020**, *20*, e1900303.
[26] X. Yan, Q. Chen, L. Zhu, H. Chen, D. Wei, F. Chen, Z. Tang, J. Yang, J. Zheng, *J. Mater. Chem. B* **2017**, *5*, 7683.
[27] A. S. Ruveyda Kilic, *Adv. Polym. Sci.* **2020**, *285*, 243.
[28] H. Cheng, J. L. Zhu, X. Zeng, Y. Jing, X. Z. Zhang, R. X. Zhuo, *Bioconjugate Chem.* **2009**, *20*, 481.
[29] S. Lin-Gibson, S. Bencherif, J. A. Cooper, S. J. Wetzel, J. M. Antonucci, B. M. Vogel, F. Horkay, N. R. Washburn, *Biomacromolecules* **2004**, *5*, 1280.
[30] J. D. Albright, L. Goldman, *J. Am. Chem. Soc.* **1967**, *89*, 2416.
[31] Z. Wang, *Comprehensive Organic Name Reactions and Reagents*, John Wiley, Hoboken, NJ **2009**.
[32] M. H. Zahir, M. M. Rahman, K. Irshad, M. M. Rahman, *Nanomaterials* **2019**, *9*, 1773.
[33] L. Liu, D. Liu, M. Wang, G. du, J. Chen, *Eur. Polym. J.* **2007**, *43*, 2672.
[34] S.-y. Wang, M. Tohti, J.-q. Zhang, J. Li, D.-q. Li, *Int. J. Biol. Macromol.* **2023**, *251*, 126276.
[35] F. Yu, X. Cao, J. du, G. Wang, X. Chen, *ACS Appl. Mater. Interfaces* **2015**, *7*, 24023.
[36] X. J. Liu, H. Q. Li, B. Y. Zhang, Y. J. Wang, X. Y. Ren, S. Guan, G. Hui Gao, *RSC Adv.* **2016**, *6*, 4850.
[37] Ş. Raman et al., *Front. Chem.* **2023**, *10*, 1094981.
[38] L. Feng, L. Wang, Y. Ma, W. Duan, S. Martin-Saldaña, Y. Zhu, X. Zhang, B. Zhu, C. Li, S. Hu, M. Bao, T. Wang, Y. Zhu, F. Yang, Y. Bu, *Bioactive Mater.* **2023**, *27*, 82.
[39] J. Hwang, P. L. Thi, S. Lee, E.-H. Park, E. Lee, E. Kim, K. Chang, K. D. Park, *J. Ind. Eng. Chem.* **2022**, *109*, 372.

SUPPORTING INFORMATION

Additional supporting information can be found online in the Supporting Information section at the end of this article.

How to cite this article: M. Yasar, B. Oktay, A. C. Gurkan, N. K. Apohan, *J. Polym. Sci.* **2024**, 1. https://doi.org/10.1002/pol.20240198